Design of magnetic textures of nanocorrals with an extra adatom

N. P. Konstantinidis[1] and Samir Lounis[2]

[1]*Fachbereich Physik und Landesforschungszentrum OPTIMAS, Technische Universität Kaiserslautern, 67663 Kaiserslautern, Germany*

[2]*Peter Grünberg Institut and Institute for Advanced Simulation, Forschungszentrum Jülich and JARA, 52425 Jülich, Germany*

(Received 2 May 2013; revised manuscript received 11 July 2013; published 18 November 2013)

It is shown that in antiferromagnetic open or closed corrals of magnetic adatoms grown on surfaces, the attachment of a single extra adatom anywhere in the corral impacts on the geometrical topology of the nanosystem and generates complex magnetic structures when a magnetic field is applied or a magnetic coupling to a ferromagnetic substrate exists. The spin configuration of the corral can be tuned to a nonplanar state or a planar noncollinear or ferrimagnetic state by adjusting its number of sites, the location of the extra adatom, or the strength of the coupling to the ferromagnetic substrate. This shows the possibility to generate nontrivial magnetic textures with atom-by-atom engineering anywhere in the corral and not only at the edges.

DOI: 10.1103/PhysRevB.88.184414 PACS number(s): 75.75.−c, 75.30.Hx, 75.50.Ee

I. INTRODUCTION

In recent years artificial engineering of molecular nanomagnets, magnetic clusters and arrays of magnetic adatoms adsorbed on surfaces has emerged for the construction of entities with rich magnetic properties that can be constituents of nanospintronics devices.[1–8] These entities can be fabricated directly on surfaces in a bottom-up fashion with scanning tunneling microscopy (STM),[9–11] and STM is also used to directly measure their magnetic properties.[12,13] The rich magnetic properties originate in the exchange couplings between the individual magnetic moments[14–17] and are of great interest for concepts like spin-transfer torque[18–20] and spin chirality[21] on the nanoscale, as well as for potential applications in quantum computing.[22–24] The STM measurements allow precise access to the properties of the individual magnetic moments, which when combined with tailored construction of the coupling between the spins provide systems where nanomagnets with desired properties can be synthesized.[25,26] In particular, arrays of a small number of magnetic atoms on nonmagnetic metallic substrates are very promising candidates in this direction. This bottom-up approach is one of the main focus research areas of nanoscience where various atomic structures, e.g., corrals of adatoms and nanowires, are engineered atom by atom.

It has already been shown theoretically using density functional theory (DFT) that adatom nanochains can support noncollinear magnetic structures when the exchange interaction between the adatoms is antiferromagnetic (AFM) and a coupling to a ferromagnetic substrate exists.[27] In the peculiar case of Mn chains on a Ni(100) substrate, the AFM coupling within the chain competes with the ferromagnetic coupling of the chain to the substrate leading to an even-odd effect, where the magnetic texture depends crucially on the parity of the number of atoms in the chain. The Mn chain is in an AFM configuration but, if the weak ferromagnetic interaction to the substrate is turned on, the spins in the odd numbered chain retain their collinearity while the uncompensated moment of the chain aligns with that of the substrate. Even numbered chains, however, develop a more complex noncollinear ground state. This even-odd effect has been observed recently by STM in short Mn wires on a Ni(110) substrate.[28]

For such an effect a ferromagnetic substrate is required when the exchange interaction is nearest neighbor, therefore strong. However, when the exchange interaction is non-nearest neighbor, therefore weaker, for example when it is mediated by Ruderman-Kittel-Kasuya-Yosida (RKKY) interactions,[29–31] an external magnetic field can provide the necessary energy to compete with the exchange energy. Measurements with STM can be performed for both kinds of situations: magnetic nanostructures on ferromagnets or on nonmagnetic substrates. We point out that if the magnetic anisotropy energy is strong (a few meV), the RKKY interactions would not be able to create noncollinear structures, although there is competition between the involved magnetic interactions.

In this paper AFM wires or corrals with a small number of magnetic adatoms are considered, where an extra adatom is attached anywhere along the nanostructure. It is shown that one more or less adatom is crucial for the magnetic properties, and can generate planar or even noncoplanar magnetic configurations. This opens up the possibility of generating new complex magnetic structures whose accessibility depends on the precise location of the extra adatom, which is not necessarily attached at the edges of the corral, the total number of sites of the corral, and the strength of the coupling to a ferromagnetic substrate or an external magnetic field. Besides the parity of the number of adatoms in the corrals, the parity of the site to which the extra atom is attached determines not only the magnetic texture of the whole nanostructure (open or closed), but also the magnetic behavior of the edge atoms for the open corrals. This is of crucial importance for building logic gates made up of a few adatoms (see, e.g., Ref. 24). In the following we will refer to wires which are not necessarily straight as open corrals.

II. MODEL

The magnetic properties of the nanostructures are modeled with the AFM Heisenberg model (AHM). It is mainly considered at the classical level, but it is also shown that the classical results compare very well with results for typical quantum values of the magnetic moments. Previous calculations based on DFT have shown that the AHM is reliable to predict the complex magnetic texture in such nanostructures.[27] The AHM is considered for corrals of adatoms that are open or closed,

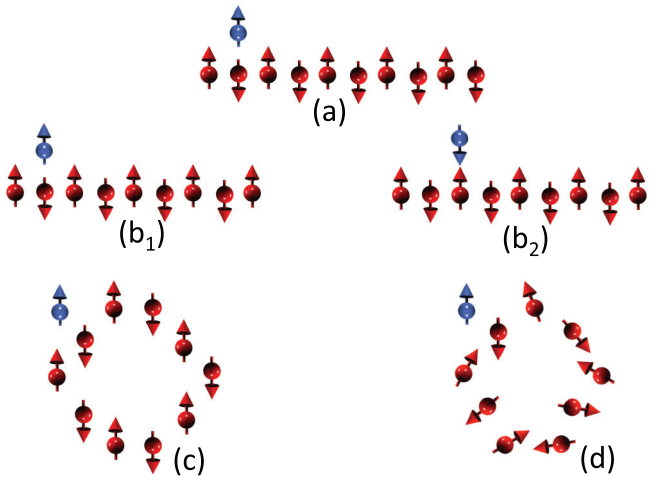

FIG. 1. (Color online) Lowest energy spin configuration for $h = 0$. (a) $N = 10$ open even corral with an extra adatom at $L = 2$. The magnetization $M_{h=0} = s$. (b1) $N = 9$ open odd corral with even $L = 2$, $M_{h=0} = 2s$. (b2) $N = 9$ open odd corral with odd $L = 3$, $M_{h=0} = 0$. (c) $N = 10$ closed even corral, $M_{h=0} = s$. (d) $N = 9$ closed odd corral, $M_{h=0} = s$.

with an extra adatom attached to any location other than the edges. The coupling between the individual spins $\vec{s}_i$ which have the same magnitude s is $J > 0$. The interaction with a ferromagnetic substrate or with an external magnetic field (in the case of a non-magnetic substrate) has strength h, and the Hamiltonian for an open corral is

$$H = J\left(\sum_{i=1}^{N-1}\vec{s}_i\cdot\vec{s}_{i+1} + \vec{s}_L\cdot\vec{s}_E\right) - h\left(\sum_{i=1}^{N} s_i^z + s_E^z\right), \quad (1)$$

where the corral has N atoms, with $L = 2,\ldots,N-1$ being the location of the corral adatom that couples to the extra adatom $\vec{s}_E$. For closed corrals $J\vec{s}_1\cdot\vec{s}_N$ must be added to (1) and L can be any site. $\vec{h}$ lies along the $\hat{z}$ axis and tends to make all spins parallel, in contrast to the AFM configuration supported by J. To simplify the discussion the magnetic interaction between $\vec{s}_E$ and $\vec{s}_L$ is also taken to be J, but results for weaker interaction will also be presented. For the case of RKKY interactions small magnetic anisotropy energies are required in order to observe a rich magnetic phase diagram, otherwise the adatom moments would be pinned to a collinear behavior. This is the case for Fe adatoms on a Cu(111) surface.[26] It is demonstrated that when small magnetic anisotropy energies are added to Hamiltonian (1) the effect on the magnetic behavior of the nanocorrals is negligible. Thus adatoms with low magnetic anisotropy energy, e.g., Cr or Mn, are proposed, in contrast to Co or Fe, to be deposited on different nonmagnetic substrates. Cr and Mn have weak magnetic anisotropy so that the AFM Heisenberg model without an extra anisotropy term accurately describes the magnetism of the system.

DFT calculations predict that for Cr, Mn and Fe deposited on Cu(111) the magnetic moments are respectively 4.1, 4.3, and 3.2 μ_B,[32] while Cr and Mn adatoms on a Ni(001) or a Fe(001) substrate have a magnetic moment of the order of 3.5 to 4 μ_B, which decreases when forming chains due to hybridization.[14] Thus, typically $s = 3/2$ or 2. It is sufficient to consider the $\vec{s}_i$ as classical unit vectors,[33,34] and the lowest energy configuration is found for any h.[35,36] Typical quantum values are also considered.[37,38] It has already been shown that for open chains with no extra spins attached the classical predictions survive for relatively low values of s.[39] Here similar conclusions are drawn for the dependence of the magnetic properties on s.

III. LOWEST ENERGY CONFIGURATIONS

For open corrals the exact location of the extra adatom is important, due to the lack of translational symmetry.[40] The magnetic behavior depends on the parity of N, and also on the parity of the linking location L of the extra adatom $\vec{s}_E$. For closed corrals the exact linking point is unimportant due to translational symmetry, and the magnetic behavior depends only on the parity of N.

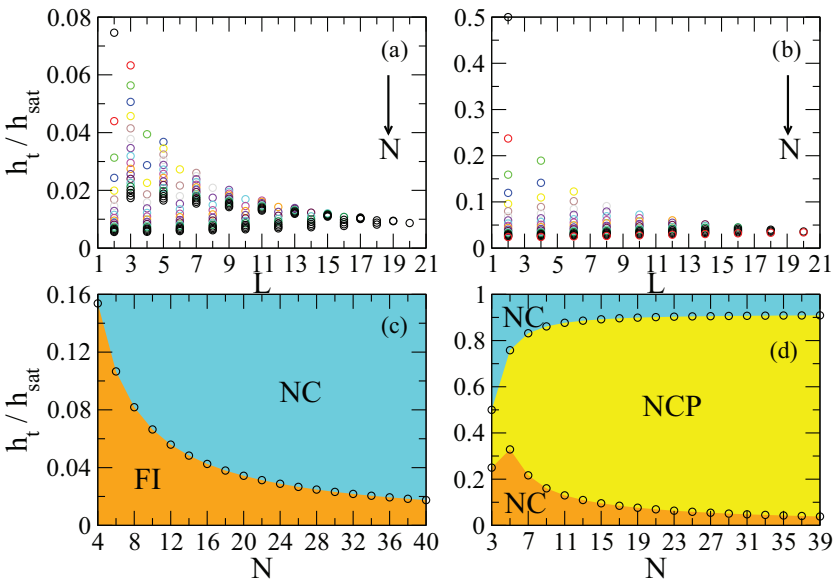

FIG. 2. (Color online) Transition fields h_t for the change from the ferrimagnetic (FI) to the planar noncollinear (NC) configuration with increasing magnetic field h, over the saturation field h_{sat}. Open corrals with (a) even N, (b) odd N. L: location of the extra adatom. $\frac{h_t}{h_{sat}}$ is symmetric with respect to the corral center. A single corral is represented by symbols of the same color. The direction where N increases is shown with the arrow. For fixed L, $\frac{h_t}{h_{sat}}$ decreases with N. For odd corrals there is a transition only for even L. Closed corrals with (c) even N, (d) odd N. NCP: noncoplanar. The configurations are distinguished by different colors.

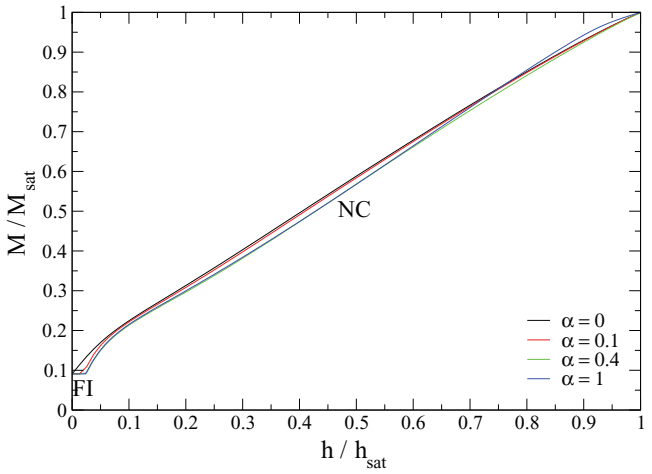

FIG. 3. (Color online) Reduced magnetization $M/M_{\rm sat}$ as a function of $h/h_{\rm sat}$ for an open corral with $N = 10$ and an extra spin linked at site $L = 9$ ($M_{\rm sat} = 11$), where the strength J of only the $\vec{s}_L \cdot \vec{s}_E$ bond in Hamiltonian (1) is scaled with α. The dependence of $M/M_{\rm sat}$ on $h/h_{\rm sat}$ does not change significantly with α. This is also true for the ferrimagnetic (FI) state, which appears for small magnetic fields when $\alpha \neq 0$ and is robust even for small values of α. NC refers to the planar noncollinear configuration.

A. Open even corrals

An open even corral with no extra adatom has nearest neighbor spins pointing in opposite directions when $h = 0$. Irrespectively of the point of attachment of the extra adatom, the extra spin is uncompensated and the total magnetization $M_{h=0} = s$, corresponding to a ferrimagnetic (FI) configuration [Fig. 1(a)]. It takes a finite field h_t to change the FI configuration, up to which the only energy gain comes from the coupling to the field. The susceptibility χ is discontinuous as h_t is crossed and for higher fields the spins are in a planar noncollinear (NC) configuration. The open even corral with an extra adatom is thus similar to an open odd chain.[39] h_t decreases on the average with N [Fig. 2(a)], as $M_{h=0}$ decreases with respect to the saturation magnetization $M_{\rm sat} = (N+1)s$ with N, $\frac{M_{h=0}}{M_{\rm sat}} = \frac{1}{N+1}$. h_t also depends on the parity of L. As L changes from even to odd, the length of the largest subchain of the corral changes its parity from even (which when isolated has no FI lowest field configuration) to odd (which possesses a FI low field configuration), and correspondingly its zero-field magnetization from 0 to s. It is thus reminiscent of an isolated even or odd chain respectively, especially since the corral feels the influence of the extra adatom more strongly around its linking site L, and its influence gradually weakens when going away from it. Therefore the length of the largest odd subchain fluctuates significantly with L when the linking point is away from the middle, generating the pronounced nonmonotonic dependence of h_t on the parity of L [Fig. 2(a)], due to the monotonic dependence of the transition field on the length for an isolated (odd) chain. When the extra adatom approaches

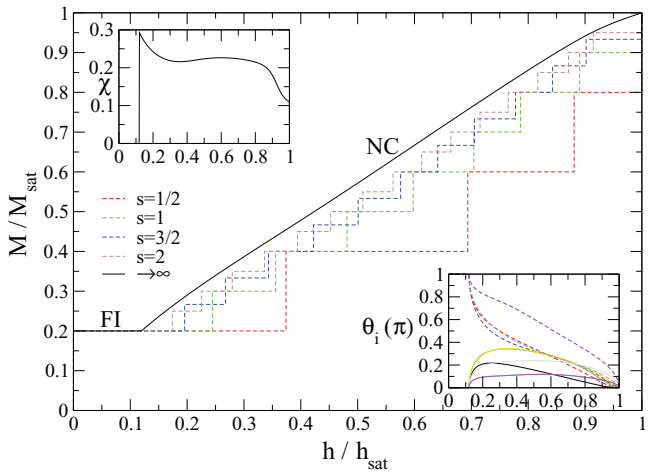

FIG. 4. (Color online) Reduced magnetization $M/M_{\rm sat}$ vs $h/h_{\rm sat}$ for an $N = 9$ open corral with extra adatom at $L = 8$ ($M_{\rm sat} = 10$). The classical configuration is ferrimagnetic (FI) for lower and planar noncollinear (NC) for higher fields. The quantum mechanical magnetization tends to the classical result as s increases from 1/2 towards the typical values 3/2 and 2. The classical susceptibility χ (upper left inset) is discontinuous at $h_t/h_{\rm sat} = 0.120$. The polar angles (lower right inset) on the average turn towards the field as it is getting stronger. For smaller fields above the discontinuity spins originally pointing along the field turn away from it to increase the exchange energy. Nearest-neighbor azimuthal angles differ by π, with the corresponding two groups of spins indicated by solid (odd-site spins and extra spin) and dashed (even-site spins) lines respectively.

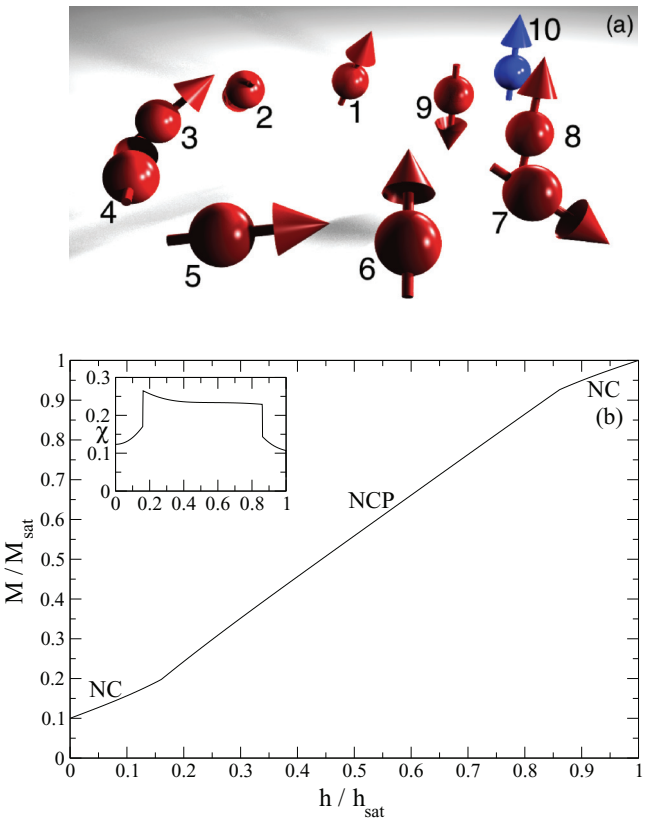

FIG. 5. (Color online) Closed $N = 9$ corral with extra adatom. (a) Noncoplanar (NCP) configuration for $h/h_{\rm sat} = 0.171$. (b) Reduced magnetization $M/M_{\rm sat}$ vs $h/h_{\rm sat}$ ($M_{\rm sat} = 10$). The susceptibility χ (inset) has discontinuities at $h_t/h_{\rm sat} = 0.160$ and 0.861, which divide the planar noncollinear (NC) configurations from the NCP.

the center of the chain the length of the largest odd subchain does not change significantly and h_t tends to a constant.

The robustness of the influence of the extra adatom on the isolated corral can be shown by varying the strength of the coupling $\vec{s}_L \cdot \vec{s}_E$, which is equal to J in Hamiltonian (1). If only this coupling is scaled with α, then the magnetization of an $N = 10$ open corral with an extra adatom attached at site $L = 9$ is shown in Fig. 3, and it does not change significantly with α. This is also true for the ferrimagnetic state, which appears for small magnetic fields when $\alpha \neq 0$ and is robust even for small values of α.

B. Open odd corrals

An open corral with an odd number of atoms has one uncompensated spin. When an extra adatom is attached $M_{h=0}$ depends on the parity of L. For even L the extra spin is parallel to the uncompensated spin of the open corral and $M_{h=0} = 2s$ [Fig. 1(b1)]. In contrast, for odd L the extra spin balances out the uncompensated spin of the corral and $M_{h=0} = 0$ [Fig. 1(b2)]. For even L the lowest energy configuration is FI, similarly to an open even corral. However there are now two uncompensated spins, consequently h_t is bigger [Fig. 2(b)]. For the same reason h_t is also bigger compared to an open even corral, which also has only a single uncompensated spin. For higher fields the lowest energy configuration is also NC, as for open even corrals (Fig. 4). The change between the FI and the NC configuration also generates a discontinuity in χ (Fig. 4, upper left inset), with nearest-neighbor spins pointing in opposite directions in the azimuthal plane above the discontinuity (Fig. 4, lower right inset). On the other hand, when L is odd, the lowest energy configuration is AFM for $h = 0$ and M immediately responds to an external field with no susceptibility discontinuity [Fig. 2(b)], leading to a NC configuration, similarly to an even corral with no extra adatoms. Consequently there are changes in the lowest energy configuration as function of h only for even L, where the size of the largest odd subchain of the isolated corral decreases with

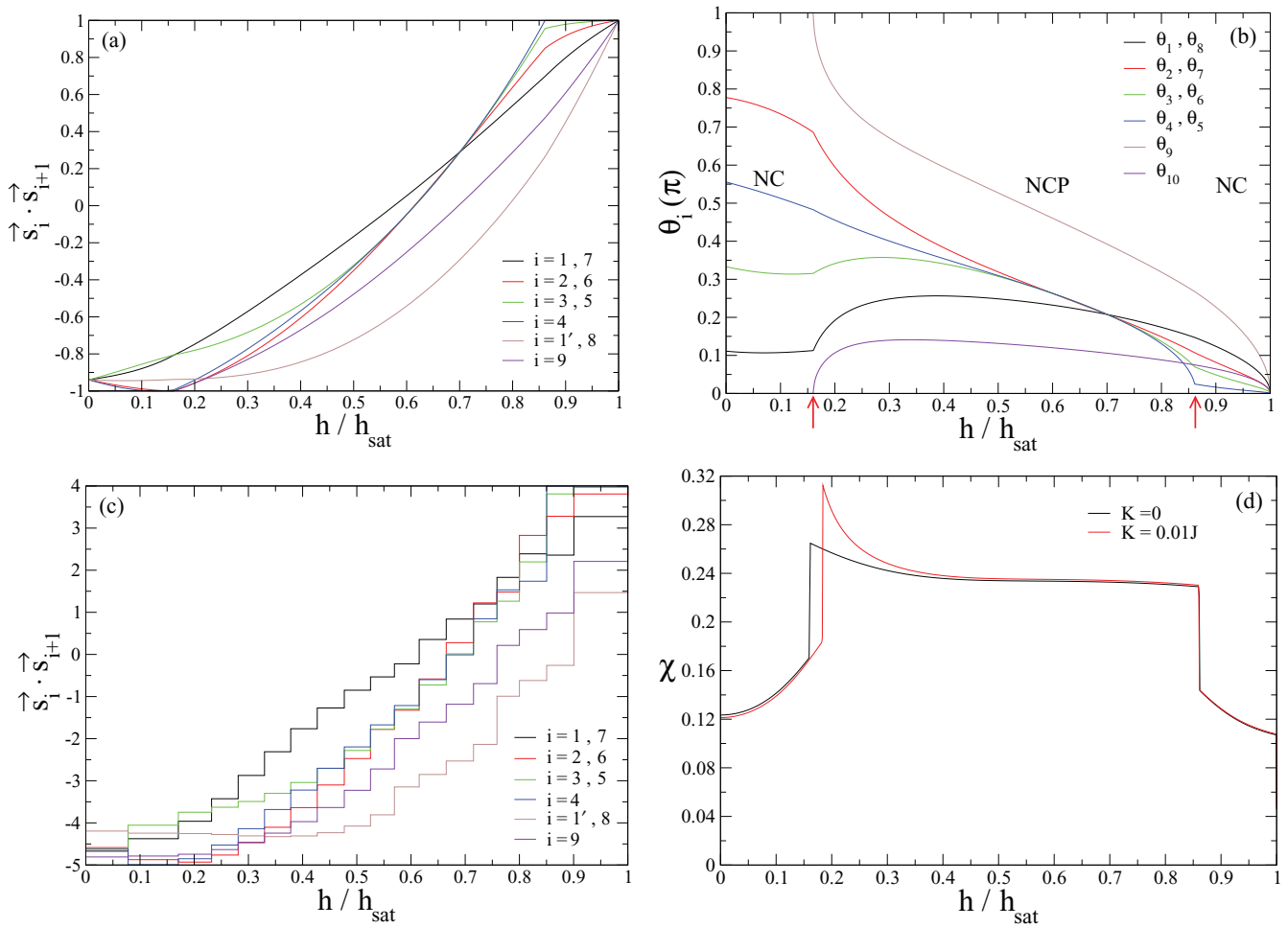

FIG. 6. (Color online) Closed $N = 9$ corral with extra adatom; the horizontal axis is $h/h_{\rm sat}$. (a) Classical nearest-neighbor correlation functions $\vec{s}_i \cdot \vec{s}_{i+1}$. $1'$ indicates $\vec{s}_1 \cdot \vec{s}_9$. (b) Polar angles in units of π. The two susceptibility discontinuities at $h_t/h_{\rm sat} = 0.160$ and 0.861 (shown with red arrows) separate the three different lowest energy configurations, which change from planar noncollinear (NC) to noncoplanar (NCP) and then to NC with increasing field. (c) Nearest-neighbor correlation functions $\vec{s}_i \cdot \vec{s}_{i+1}$ for $s = 2$. $1'$ indicates $\vec{s}_1 \cdot \vec{s}_9$. The results are similar to the classical results [compare with (a)]. (d) Magnetic susceptibility χ without and with magnetic anisotropy K, with the easy axis parallel to the direction of the magnetic field. A small $K = 0.01J$ does not change significantly the magnetic response. The two susceptibility discontinuities are now at $h_t/h_{\rm sat} = 0.184$ and 0.861.

L. Thus the transition field for increasing even L increases as the zero-field subchain magnetization increases with respect to the saturation magnetization of the subchain, in contrast to the nonmonotonic result of open even corrals. This shows the importance of the exact location of attachment of the extra adatom for the magnetic configuration, leading to an even-odd linking effect for open odd corrals, which is absent for open even corrals. These clear-cut differences between open even and open odd corrals provide the opportunity for a variety of magnetic structures as the length of the corral is varied and the extra adatom is moved along the corral with STM.

Up to now, classical spins have been considered in Hamiltonian (1). However, typically $s = 3/2$ or 2 and magnetization curves for $s \leqslant 2$ are shown in Fig. 4. The quantum mechanical magnetization approaches the classical with increasing s, quite close already for $s = 2$. Therefore the qualitative features of the classical calculation are expected to survive for actual s values, in accordance with open chains.[39]

C. Closed even corrals

In a closed corral due to translational invariance the exact linking point L of the extra adatom does not affect the magnetic behavior. For an isolated even corral there is no frustration originating in the closed boundary conditions, and nearest neighbor spins are antiparallel with no net magnetization in the abscence of a field [Fig. 1(c)]. The extra adatom provides an uncompensated spin and $M_{h=0} = s$, and it takes a finite magnetic field to destroy the FI configuration and generate a NC one, similarly to the previous cases. In the NC state spins symmetrically placed with respect to the linking adatom $\vec{s}_L$ point in the same direction. The dependence of h_t on N is shown in Fig. 2(c). As was the case before, $M_{h=0}$ decreases with respect to $M_{\rm sat}$ as $1/(N+1)$, thus h_t decreases with N.

D. Closed odd corrals

For odd N the periodic boundary condition introduces a frustrated configuration even for an isolated closed corral with no extra adatoms.[41,42] It is not possible for nearest-neighbor spins to be antiparallel even when $h = 0$; however, the net magnetization is still zero. The extra adatom provides an uncompensated spin and $M_{h=0} = s$, but the configuration now is NC, unlike the FI configurations found before [Fig. 1(d)]. This configuration is susceptible to an infinitesimal magnetic field, again unlike all previous cases with $M_{h=0} \neq 0$ [Fig. 5(b)]. In it the extra and the linking adatom are always antiparallel, with the extra adatom being parallel and the linking adatom antiparallel to the field. Spins which are symmetrically placed with respect to the linking adatom $\vec{s}_L$ have the same polar angle (this is true for all magnetic fields up to saturation), but they point in opposite directions in the azimuthal plane [Fig. 6(b)]. In addition, nearest-neighbor correlations between specific pairs of spins increase with h, and eventually these spins become antiparallel [Fig. 6(a)]. These pairs are arranged in a "dimer" type of configuration, with every second bond increasing or decreasing in correlation strength. From the ones which are getting stronger with h, they increase in correlation strength as the linking point L of the extra adatom is approached. This is counterintuitive and points to the importance of the single extra spin for the change of the magnetic properties of the whole corral.

With increasing field, a susceptibility discontinuity leads for the first time to a noncoplanar (NCP) lowest spin configuration [Fig. 5(b)], shown in Fig. 5(a) for $h/h_{\rm sat} = 0.171$. The nearest-neighbor correlations now only decrease with the magnetic field [Fig. 6(a)], even though there are initially polar angles that do not decrease with h, due to the competition of exchange and magnetic energy [Fig. 6(b)]. For higher fields close to saturation a second susceptibility discontinuity leads to a NC configuration [Fig. 5(b)]. Now spins symmetrically placed with respect to the linking adatom $\vec{s}_L$ point in the same direction. The transition fields and the range of existence of the different configurations as function of N are shown in Fig. 2(d). The odd closed corral with the extra adatom combines the competition between exchange and magnetic energy with the frustration introduced by the closed boundary conditions, supporting a NCP configuration not found in any of the other cases. In addition, it supports two susceptibility discontinuities in its magnetization curve. Therefore its magnetic behavior is in direct contrast with its even counterpart and the open corrals as well.

The nearest-neighbor correlations for the typical quantum spin $s = 2$ are shown in Fig. 6(c), where by comparison with Fig. 6(a) it is seen that the classical result again provides a very good description. The influence of weak easy-axis magnetic anisotropy can be seen in Fig. 6(d), where a term $-K[\sum_{i=1}^{N}(s_i^z)^2 + (s_E^z)^2]$ is added in Hamiltonian (1), with the easy axis parallel to the magnetic field axis. For weak anisotropy $K = 0.01J$ the magnetic response does not change significantly.

IV. CONCLUSIONS

The magnetic properties of corrals (open or closed) with an extra adatom attached are different from their counterparts without the extra adatom. The extra spin changes the geometrical topology of the nanosystem, which has an impact on its magnetic behavior as a whole. It can tune the lowest energy configuration of the spins according to the parity of the corral, the parity of the linking point of the extra spin, and the presence or not of periodic boundary conditions. This leads to a plethora of configurations that can also be three-dimensional, and can be accessed and of use experimentally.

ACKNOWLEDGMENTS

N.P.K. acknowledges support by the Graduate School of Excellence MAINZ. S.L. acknowledges the support of the HGF-YIG Program No. VH-NG-717 (Functional nanoscale structure and probe simulation laboratory-Funsilab).

[1] J. P. Bucher, D. C. Douglass, and L. A. Bloomfield, Phys. Rev. Lett. **66**, 3052 (1991).

[2] J. T. Lau, A. Föhlisch, R. Nietubyć, M. Reif, and W. Wurth, Phys. Rev. Lett. **89**, 057201 (2002).

[3]H. Manoharan, C. Lutz, and D. Eigler, Nature (London) **403**, 512 (2000).
[4]P. Gambardella, A. Dallmeyer, K. Maiti, M. C. Malagoli, W. Eberhardt, K. Kern, and C. Carbone, Nature (London) **416**, 301 (2002).
[5]N. Knorr, H. Brune, M. Epple, A. Hirstein, M. A. Schneider, and K. Kern, Phys. Rev. B **65**, 115420 (2002).
[6]F. Silly, M. Pivetta, M. Ternes, F. Patthey, J. P. Pelz, and W.-D. Schneider, Phys. Rev. Lett. **92**, 016101 (2004).
[7]C. F. Hirjibehedin, C. P. Lutz, and A. J. Heinrich, Science **312**, 1021 (2006).
[8]S. Loth, S. Baumann, C. P. Lutz, D. M. Eigler, and A. J. Heinrich, Science **335**, 196 (2012).
[9]D. M. Eigler and E. K. Schweizer, Nature (London) **344**, 524 (1990).
[10]F. J. Rueß, W. Pok, T. C. G. Reusch, M. J. Butcher, K. E. J. Goh, L. Oberbeck, G. Scappucci, A. R. Hamilton, and M. Y. Simmons, Small **3**, 563 (2007).
[11]C. R. Moon, L. S. Mattos, B. K. Foster, G. Zeltzer, and H. C. Manoharan, Nat. Nanotechnol. **4**, 167 (2009).
[12]F. Meier, L. Zhou, J. Wiebe, and R. Wiesendanger, Science **320**, 82 (2008).
[13]A. J. Heinrich, J. A. Gupta, C. P. Lutz, and D. M. Eigler, Science **306**, 466 (2004).
[14]S. Lounis, P. Mavropoulos, P. H. Dederichs, and S. Blügel, Phys. Rev. B **72**, 224437 (2005).
[15]M. S. Ribeiro, G. B. Corrêa, A. Bergman, L. Nordström, O. Eriksson, and A. B. Klautau, Phys. Rev. B **83**, 014406 (2011).
[16]V. S. Stepanyuk, L. Niebergall, W. Hergert, and P. Bruno, Phys. Rev. Lett. **94**, 187201 (2005).
[17]A. Bergman, L. Nordström, A. B. Klautau, S. Frota-Pessôa, and O. Eriksson, Phys. Rev. B **73**, 174434 (2006).
[18]J. C. Slonczewski, J. Magn. Magn. Mater. **159**, L1 (1996).
[19]S. I. Kiselev, J. C. Sankey, I. N. Krivorotov, N. C. Emley, R. J. Schoelkopf, R. A. Buhrman, and D. C. Ralph, Nature (London) **425**, 380 (2003).
[20]S. Krause, L. Berbil-Bautista, G. Herzog, M. Bode, and R. Wiesendanger, Science **317**, 1537 (2007).
[21]M. Menzel, Y. Mokrousov, R. Wieser, J. E. Bickel, E. Vedmedenko, S. Blügel, S. Heinze, K. von Bergmann, A. Kubetzka, and R. Wiesendanger, Phys. Rev. Lett. **108**, 197204 (2012).
[22]M. N. Leuenberger and D. Loss, Nature (London) **410**, 789 (2001).
[23]F. Troiani, A. Ghirri, M. Affronte, S. Carretta, P. Santini, G. Amoretti, S. Piligkos, G. Timco, and R. E. P. Winpenny, Phys. Rev. Lett. **94**, 207208 (2005).
[24]A. A. Khajetoorians, J. Wiebe, B. Chilian, and R. Wiesendanger, Science **332**, 1062 (2011).
[25]L. Zhou, J. Wiebe, S. Lounis, E. Vedmedenko, F. Meier, S. Blügel, P. H. Dederichs, and R. Wiesendanger, Nature Phys. **6**, 187 (2010).
[26]A. A. Khajetoorians, J. Wiebe, B. Chilian, S. Lounis, S. Blügel, and R. Wiesendanger, Nature Phys. **8**, 497 (2012).
[27]S. Lounis, P. H. Dederichs, and S. Blügel, Phys. Rev. Lett. **101**, 107204 (2008).
[28]S. Holzberger, T. Schuh, S. Blügel, S. Lounis, and W. Wulfhekel, Phys. Rev. Lett. **110**, 157206 (2013).
[29]M. A. Ruderman and C. Kittel, Phys. Rev. **96**, 99 (1954).
[30]T. Kasua, Prog. Theor. Phys. **16**, 45 (1956).
[31]K. Yosida, Phys. Rev. **106**, 893 (1957).
[32]S. Lounis, P. Mavropoulos, P. H. Dederichs, and S. Blügel, Phys. Rev. B **73**, 195421 (2006).
[33]J. H. Luscombe, M. Luban, and F. Borsa, J. Chem. Phys. **108**, 7266 (1998).
[34]D. Mentrup, H.-J. Schmidt, J. Schnack, and M. Luban, Physica A **278**, 214 (2000).
[35]D. Coffey and S. A. Trugman, Phys. Rev. Lett. **69**, 176 (1992).
[36]N. P. Konstantinidis, Phys. Rev. B **76**, 104434 (2007).
[37]N. P. Konstantinidis, Phys. Rev. B **72**, 064453 (2005).
[38]N. P. Konstantinidis, Phys. Rev. B **80**, 134427 (2009).
[39]A. Machens, N. P. Konstantinidis, O. Waldmann, I. Schneider, and S. Eggert, Phys. Rev. B **87**, 144409 (2013).
[40]E. Micotti, Y. Furukawa, K. Kumagai, S. Carretta, A. Lascialfari, F. Borsa, G. A. Timco, and R. E. P. Winpenny, Phys. Rev. Lett. **97**, 267204 (2006).
[41]K. Bärwinkel, H.-J. Schmidt, and J. Schnack, J. Magn. Magn. Mater. **220**, 227 (2000).
[42]J. Schnack, Dalton Trans. **39**, 4677 (2010).